

# Deep learning-based sequential data assimilation for chaotic dynamics identifies local instabilities from single state forecasts

Marc Bocquet,<sup>1, a)</sup> Alban Farchi,<sup>1</sup> Tobias S. Finn,<sup>1</sup> Charlotte Durand,<sup>1</sup> Sibo Cheng,<sup>1</sup> Yumeng Chen,<sup>2</sup> Ivo Pasmans,<sup>2</sup> and Alberto Carrassi<sup>3</sup>

<sup>1)</sup>*CEREA, École des Ponts and EDF R&D, Île-de-France, France*

<sup>2)</sup>*Department of Meteorology and National Centre for Earth Observation, University of Reading, Earley Gate, PO Box 243, Reading, RG6 6BB, United Kingdom*

<sup>3)</sup>*Department of Physics and Astronomy, University of Bologna, Viale Carlo Berti Pichat, 6/2, Bologna, 40127, Italy*

(\*Electronic mail: marc.bocquet@enpc.fr.)

(Dated: 12 August 2024)

We investigate the ability to discover data assimilation (DA) schemes meant for chaotic dynamics with deep learning (DL). The focus is on learning the analysis step of sequential DA, from state trajectories and their observations, using a simple residual convolutional neural network, while assuming the dynamics to be known. Experiments are performed with the Lorenz 96 dynamics, which display spatiotemporal chaos and for which solid benchmarks for DA performance exist. The accuracy of the states obtained from the learned analysis approaches that of the best possibly tuned ensemble Kalman filter (EnKF), and is far better than that of variational DA alternatives. Critically, this can be achieved while propagating even just a single state in the forecast step. We investigate the reason for achieving ensemble filtering accuracy without an ensemble. We diagnose that the analysis scheme actually identifies key dynamical perturbations, mildly aligned with the unstable subspace, from the forecast state alone, without any ensemble-based covariances representation. This reveals that the analysis scheme has learned some multiplicative ergodic theorem associated to the DA process seen as a non-autonomous random dynamical system.

**Data assimilation (DA) estimates the state of dynamical systems from sparse and noisy observations, and is used worldwide in numerical weather prediction centers. Accurate DA demands the representation of the time-dependent errors in this state estimate, usually achieved through the propagation of an ensemble of states. Using deep learning, we discover the update step of DA applied to chaotic dynamics. We show that a simple convolutional neural network (CNN) can learn DA, reaching an accuracy as good as that of ensemble-based DA. Crucially, the CNN can achieve this best accuracy with single state forecasts. This is explained by the CNN's ability to identify local space patterns from this one state, which are used to assess the errors in the analysis. This suggests building a new class of efficient DL-based ensemble-free DA algorithms.**

## I. INTRODUCTION

### A. Sequential data assimilation and accuracy

Sequential data assimilation (DA) is a set of algorithms required to accurately track the trajectory of chaotic dynamics, using a dynamical model and imperfect observations. It is widely used in numerical weather prediction (NWP), and in many areas of climate sciences,<sup>1</sup> as a suite of both research and operational tools. Classical DA methods are

classified into (i) variational methods, such as 3D-Var and 4D-Var, (ii) ensemble-based statistical methods, such as the ensemble Kalman filter (EnKF), and (iii) ensemble variational methods which inherit the assets of the two previous categories.<sup>2</sup> On the one hand, variational methods account for the nonlinearity of models (dynamical model and observation operators), leveraging nonlinear optimization techniques. Ensemble-based methods on the other hand can capture the *errors of the day*, i.e. time-dependent error statistics, via an ensemble meant to diagnose sample error statistics. Those are key properties that drive the performance of these DA methods in mildly nonlinear chaotic models. For low-order, chaotic dynamics such as the celebrated Lorenz 96 (L96) model,<sup>3</sup> the EnKF significantly outperforms 3D-Var, or a moderately-long window 4D-Var in terms of accuracy, owing to its dynamical representation of the errors. This has been emphasized and illustrated in twin experiments.<sup>4</sup> In fact, current implementations of 4D-Var in NWP centers, incorporate a forecast ensemble so as to capture the errors-of-the-day.<sup>5,6</sup> However, in high-dimensional models, these ensemble-based error statistics must necessarily be regularized using techniques known as localization and possibly inflation.<sup>7</sup>

### B. Time-dependent error statistics and dynamical systems

With a focus on the time-dependent error statistics of sequential DA, it has been conjectured<sup>8,9</sup> then proven<sup>10–12</sup> that for linear dynamics and when localization is unnecessary, the forecast and analysis error covariance matrices of the EnKF are confined to the unstable-neutral subspace, denoted as  $\mathcal{U}$  from now on, of the dynamics. This subspace is spanned by the covariant Lyapunov vectors associated to non-negative

<sup>a)</sup><https://cerEA.enpc.fr/HomePages/bocquet/>

Lyapunov exponents.<sup>13</sup> It is precisely when the ensemble size is smaller than the dimension of this subspace that localization is required to avoid divergence of the EnKF. Deviating from linear dynamics turns those exact results into approximations, for which these findings were nonetheless numerically confirmed.<sup>14–16</sup>

### C. End-to-end data assimilation and deep learning

This paper focuses on methodological DA and on what can be discovered from deep learning (DL) techniques to improve state-of-the-art DA schemes such as those mentioned above. Hence, we hereby give a brief account on the recent introduction of DL techniques for DA applied to chaotic dynamics.<sup>17</sup>

It was first proposed to learn DA analysis through DL from the data produced by existing DA schemes.<sup>18,19</sup> One can alternatively replace the solver of a 4D-Var over a long DA window by a DL operator that would learn the outcome of the 4D-Var cost function minimization.<sup>20–24</sup> However, the latter approaches do not consider cycling sequential DA, the focus of the present paper. A systematic, formal Bayesian view on the use of DL in the critical components of sequential DA has been proposed<sup>25</sup> and called *data assimilation network* (DAN). In the present paper, a simplified variant of this DAN concept is used. As far as ensemble and Kalman-related DA methods are concerned, it has been proposed to learn their Kalman gain,<sup>26,27</sup> or parameters thereof, possibly relying on an auto-differentiable implementation of the (En)KF.<sup>28–30</sup> A step further, it was also proposed to learn the fully analysis operator using (self-)supervision.<sup>25,31</sup> Finally, bypassing the need for dynamical models and DA schemes altogether, DL-based *end-to-end* methods aim at estimating states of the system from the observations only,<sup>32,33</sup> but with a focus on the feasibility of such endeavor for now.

### D. Objective

In this paper, the forecast model is assumed to be known so as to disentangle intricate interactions of learning simultaneously the DA operators and the dynamics altogether. Our objective is to learn the analysis step of a sequential DA scheme meant for chaotic dynamics from a long trajectory of the dynamical system and the associated set of noisy, potentially partial observations. Supervised learning is used although self-supervised learning<sup>31,34,35</sup> could have been used instead but is more challenging and rather disconnected from the main results of this paper. The (incremental) analysis CNN operator will be referred to as  $a_\theta$ , while the full resulting DA scheme will be called DAN.

We will show that the learned  $a_\theta$  directly discovers and utilizes a fine knowledge of the dynamics, as opposed to agnostic classical DA. The nature of these fine dynamical structures learned through  $a_\theta$  will then be discussed and interpreted, together with key implications for the development of modern DA methods.

## II. EXPERIMENTAL SETUP

We use a twin experiment setup where the states of a trajectory of the dynamics,  $\mathbf{x}_k^t \in \mathbb{R}^{N_x}$  at equally spaced times  $t_k$  for  $k = 1 \dots N_c$ , are generated from the known dynamics; the superscript “ $t$ ” stands for truth. A set of observation vectors  $\mathbf{y}_k \in \mathbb{R}^{N_{y,k}}$  are obtained from these states  $\mathbf{x}_k^t$  via an observation operator  $\mathcal{H}_k$ , and perturbed by a white-in-time Gaussian noise  $\varepsilon_k$  of mean  $\mathbf{0}$  and covariance matrix  $\mathbf{R}_k \in \mathbb{R}^{N_{y,k} \times N_{y,k}}$ :

$$\mathbf{y}_k = \mathcal{H}_k(\mathbf{x}_k^t) + \varepsilon_k, \quad \varepsilon_k \sim N(\mathbf{0}, \mathbf{R}_k). \quad (1)$$

### A. Analysis operator and its neural network representation

Let us define a sequential DA scheme, based on an analysis and forecast (also called background) ensemble. The  $i$ -th members of the analysis and forecast ensembles at time  $t_k$  are noted  $\mathbf{x}_k^{a,i}$  and  $\mathbf{x}_k^{f,i}$ , respectively. Denoting  $\mathcal{S}_e = 1 \dots N_e$ , the corresponding analysis and forecast ensembles are  $\mathbf{E}_k^a = \left\{ \mathbf{x}_k^{a,i} \right\}_{i \in \mathcal{S}_e} \subset \mathcal{E}^e$ ,  $\mathbf{E}_k^f = \left\{ \mathbf{x}_k^{f,i} \right\}_{i \in \mathcal{S}_e} \subset \mathcal{E}^e$ , respectively, where  $\mathcal{E}^e = \mathbb{R}^{N_e \times N_x}$ . The initial ensemble  $\mathbf{E}_0^f$  is obtained from perturbing a random state on the attractor of the dynamics.

The analysis step of the DA scheme is given by the (incremental) analysis operator  $a_\theta$ , which depends on a set of CNN weights and biases, a vector  $\theta$ ,

$$\mathbf{E}_k^a = \mathbf{E}_k^f + a_\theta \left( \mathbf{E}_k^f, \mathbf{H}_k^T \mathbf{R}_k^{-1} \delta_k \right), \quad (2a)$$

where  $\delta_k$ , the innovation at time  $t_k$ , is defined by

$$\delta_k \stackrel{\Delta}{=} \mathbf{y}_k - \mathcal{H}_k \left( \bar{\mathbf{x}}_k^f \right), \quad \bar{\mathbf{x}}_k^f \stackrel{\Delta}{=} \frac{1}{N_e} \sum_{i \in \mathcal{S}_e} \mathbf{x}_k^{f,i}. \quad (2b)$$

$\mathbf{H}_k$  is the tangent linear operator of  $\mathcal{H}_k$  but any arbitrary injective operator from  $\mathbb{R}^{N_{y,k}}$  to  $\mathbb{R}^{N_x}$  could be chosen instead. The DA forecast step propagates the analysis ensemble,

$$\mathbf{E}_{k+1}^f = \mathcal{M}(\mathbf{E}_k^a), \quad (3)$$

member-wise;  $\mathcal{M}$  is the resolvent over  $t_{k+1} - t_k$  of the autonomous, i.e. time-independent, dynamics.

In this paper, we choose  $a_\theta$  to be a simple residual CNN, whose architecture is detailed in Appendix A. The internal convolutional layers are chosen to have  $N_f$  channels. Hence, the internal state of the CNN consists of  $N_f$  copies of the latent space which we simply chose to be isomorphic to the state space  $\mathbb{R}^{N_x}$ . Furthermore, the encoder and decoder from state space to latent space and back, are chosen to coincide with the identity.

### B. Training scheme

Towards efficiently learning an optimal  $a_\theta$ , we consider  $N_r$  such DA runs, based on as many independent concurrent trajectories of the dynamics and as many sequences of

observation vectors. The DA runs are hence specified by  $\mathbf{E}_k^{a,r} = \left\{ \mathbf{x}_k^{a,i,r} \right\}_{i \in \mathcal{S}_e}$  and  $\mathbf{E}_k^{f,r}$  for  $r = 1 \dots N_r$  and, being iterates through  $N_c$  cycles, they depend on  $\theta$ , except for the set of initial conditions  $\mathbf{E}_0^{f,r}$ . In order to learn an optimal  $a_\theta$ , a loss function is defined:

$$\mathcal{L}(\theta) = \sum_{r=1}^{N_r} \sum_{k=1}^{N_c} \left\| \mathbf{x}_k^{t,r} - \bar{\mathbf{x}}_k^{a,r}(\theta) \right\|^2, \quad \bar{\mathbf{x}}_k^{a,r} \triangleq \frac{1}{N_e} \sum_{i \in \mathcal{S}_e} \mathbf{x}_k^{a,i,r}, \quad (4)$$

where  $\|\cdot\|$  is the Euclidean norm. This loss matches the analysis ensemble mean trajectory with the true trajectory. The Adam stochastic gradient descent optimization technique<sup>36</sup> is used to minimize it. To avoid the risks of exploding gradients, the inefficiency of vanishing gradients, and huge memory requirements, when computing gradients of Eq. (4), the truncated backpropagation through time technique<sup>37,38</sup> is used; it splits the trajectories in the dataset into chunks of  $N_{\text{iter}}$  cycles.

It must be pointed out that a proper sequential DA process when seen as a dynamical system, is stable.<sup>39,40</sup> Hence, after a rough starting phase in the training, the learned  $a_\theta$  should yield a numerically stable prediction-assimilation dynamical system. In particular, this is likely to avoid exploding gradients. By contrast, the task of learning a DL emulator of the dynamics over many consecutive time steps fails because of the unstable nature of the chaotic dynamics.

The  $N_r$  trajectories are dispatched into a training and validation dataset with a 90% – 10% ratio. Moreover, the testing dataset is generated from an independently generated trajectory, long enough to yield converged statistics. In the test stage, the DAN scheme is used within a twin experiment using the trajectories and resulting observations of the testing dataset. Its performance is assessed using the time-averaged root mean square error (aRMSE) against the truth.

### III. NUMERICAL RESULTS

The  $a_\theta$  operator is trained on the L96 model, and the results will be interpreted and discussed in the context of this model. The L96 model is a one-dimensional model defined over a periodic band of latitude of the Earth atmosphere. Its ordinary differential equations read

$$\frac{dx_n}{dt} = (x_{n+1} - x_{n-2})x_{n-1} - x_n + F, \quad (5)$$

where  $x_{N_x} = x_0$ ,  $x_{-1} = x_{N_x-1}$ ,  $x_{-2} = x_{N_x-2}$ ,  $F = 8$ , and  $N_x = 40$  in the basic configuration. The Lyapunov time of this model is 0.60; it has 13 positive Lyapunov exponents and a zero Lyapunov exponent as a continuous-in-time autonomous system. Hence, the dimension of  $\mathcal{U}$  is  $N_u = 14$ .

#### A. Hyperparameters sensitivity analysis

We first carry out a large set of trainings to assess the sensitivity of  $a_\theta$ 's performance to its hyperparameters. We chose  $N_{\text{iter}} = 16$ , without any significant gain beyond this

value while the numerical cost increases due to a deeper back-propagation. We assume the model to be fully observed with  $\mathcal{H} = \mathbf{I}_x$ , the identity matrix in  $\mathbb{R}^{N_x}$ , and the observations to be affected by a white-in-time unbiased Gaussian noise of covariance matrix  $\mathbf{R} = \mathbf{I}_x$ , for all time steps. This configuration is very often used to benchmark new DA schemes. The ensemble size  $N_e$  and the number of filter  $N_f$  were selected in a set ranging between 1 and 40. The number  $N_b$  of residual blocks in the CNN and number of subblocks  $N_{\text{sb}}$  in each residual block were both chosen in the set  $\llbracket 1, 6 \rrbracket$ . Because the L96 model has short-range correlations in space, we choose a kernel size of  $f_v = 5$ , even though the CNN receptive field is much larger. Overfitting is prevented by an early stopping of the minimization based on the validation score.

#### B. First results and robustness

The test DA runs with the trained  $a_\theta$  are actually all stable in time, yielding an aRMSE significantly below 1, as expected if DA has any skill over the mere observations.

Unsurprisingly, we found that the larger the hyperparameters  $N_f, N_b, N_{\text{sb}}$ , the smaller the test aRMSEs of the resulting DANs, but that  $N_f = 40$ ,  $N_b = 5$ , and  $N_{\text{sb}} = 5$  offer a good compromise for accuracy versus training cost and CNN size. This will be the reference configuration.

One obvious essential drawback of learning  $a_\theta$  is its *non-universality*. Specifically,  $a_\theta$  depends on the observation setup used in the training dataset. This is a critical research path for end-to-end DA. Although not the aim of the present paper, we nonetheless checked the performance of the trained  $a_\theta$ , with  $\mathcal{H} = \mathbf{I}_x$  and  $\mathbf{R} = \sigma_y^2 \mathbf{I}_x$  with  $\sigma_y = 1$ , in test DA runs with similar observations but generated with  $\sigma_y$  taking value in between 0.1 and 3.2. Yet, in all test runs, DAN remains robust with slightly degraded aRMSEs for  $\sigma_y < 1$  but aRMSEs at least as good for  $\sigma_y > 1$ , compared to a well-tuned EnKF. Well-tuned EnKF always refers here to an EnKF with an ensemble large enough such that localization is unnecessary and relying on the EnKF-N<sup>41,42</sup> to optimally counteract residual sampling errors such that inflation is unnecessary. We also learned a unique  $a_\theta$  from observation networks whose density  $N_y/N_x$  is randomly and uniformly chosen in the interval  $[0, 1]$ , and  $\sigma_y = 1$ . This DAN was then tested on several DA runs, each one with a fixed observation density  $N_y/N_x$  taking value in the interval  $[0.2, 1]$ . In this configuration,  $a_\theta$  performs almost as well or better than well-tuned EnKFs for  $0.35 < N_y/N_x < 0.65$  and is suboptimal (compared to the EnKF) but still stable outside of this range. These results already pleasantly suggest that the findings that follow may remain valid well beyond the specifications of observation operators from which  $a_\theta$  was learned.

#### C. One state forecast

Using the reference configuration but with an ensemble size  $N_e$  taking values in the set  $\llbracket 1, 40 \rrbracket$ , test aRMSEs fluctuate in between 0.19 and 0.20. By contrast, a sizable ensemble is,

as we recalled in Sec. I, one of the key reason for the success of the EnKF. For quantitative comparison, we checked that 3D-Var scores an aRMSE of 0.40, the best linear filter, i.e.  $a_\theta$  learned without activation functions scores 0.38, whereas well-tuned EnKFs with  $N_e = 20$  and  $N_e = 40$  score 0.191 and 0.179, respectively. Note that the reference  $a_\theta$  but with  $N_f = 100$  yields an aRMSE of 0.185, closer to the best EnKF with  $N_e = N_x = 40$ , showing that further improvements are possible even though not the focus of this paper.

However, the key remark is that a single state forecast,  $N_e = 1$  in  $a_\theta$ , is as efficient as using a large ensemble. Furthermore, the need for localization and inflation is completely obviated. We have checked that this is obtained concurrently to a feature collapse in  $a_\theta$ ,<sup>43</sup> i.e. all channels' last layer feature maps converge to the same state. It is likely that a better local minimum of the loss could be obtained with complex encoder and decoder<sup>44</sup> and infusing diversity in the NN through Monte Carlo dropouts,<sup>31</sup> so as to obtain an  $a_\theta$  leveraging the ensemble. Nonetheless, the local minimum reached in our trainings, yield an accuracy with  $N_e = 1$  worthy of a well-tuned EnKF. That is why we shall concentrate in the following on interpreting this astonishing result, especially in Sec. IV, using dynamical systems theory.

Consequently, the analysis operator is hereafter learned in the reference configuration but with  $N_e = 1$ .

#### IV. INTERPRETATION AND SUPPORTING RESULTS

In this section, we focus on the main result: a learned DA method with a single state forecast achieves performance on par with a well tuned EnKF. We would like to understand the reason for this performance and what  $a_\theta$  is learning.

##### A. Kalman gain-based expansion

Towards this goal, we build an incremental classical Kalman update<sup>45,46</sup> that would be a good match to  $a_\theta$  seen as a mathematical map, at least for small analysis increments. The first diagnostic is the mean anomaly generated by  $a_\theta$ , i.e. how much  $a_\theta(\mathbf{x}, \mathbf{0})$  deviates from  $\mathbf{0}$  on average. It should be small since a vanishing innovation  $\delta_k$  should not yield any state update. Hence, we define the time-dependent normalized scalar anomalies

$$b_k = \frac{1}{\sqrt{N_x}} \|a_\theta(\mathbf{x}_k, \mathbf{0})\|, \quad (6)$$

along with the associated mean bias  $b$  and the standard deviation  $s$  of  $b_k$  in time.

Next, expanding with respect to the innovation, the following functional form for  $a_\theta$  is assumed:

$$a_\theta(\mathbf{x}, \mathbf{H}^\top \mathbf{R}^{-1} \delta) \approx \mathbf{K}(\mathbf{x}) \cdot \delta, \quad (7)$$

owing to the fact that no state update is needed when the innovation vanishes, and only keeping the leading order term in  $\delta$ . This is an Ansatz of  $a_\theta$  where  $\mathbf{K}(\mathbf{x}) \in \mathbb{R}^{N_x \times N_y}$  is meant

to stand as a Kalman gain surrogate. With the propagation of a single state, classical sequential DA methods would typically resemble 3D-Var, and the gain would not depend on the forecast state (the first input variable of  $a_\theta$ ). The 3D-Var equivalent gain would be

$$\mathbf{K}_{3D-Var} = \mathbf{B} \mathbf{H}^\top (\mathbf{R} + \mathbf{B} \mathbf{H} \mathbf{H}^\top)^{-1}, \quad (8)$$

where  $\mathbf{R}$  and/or  $\mathbf{H}$  might depend on time if the monitoring system does so, and where  $\mathbf{B}$  represents some expected climatology of the DA errors.

Interestingly, we also learned  $a_\theta$  replacing Eq. (2a) with the simplified  $\mathbf{E}_k^a = \mathbf{E}_k^f + a_\theta(\mathbf{H}_k^\top \mathbf{R}_k^{-1} \delta_k)$ , whereby losing  $a_\theta$ 's ability to extract information from  $\mathbf{E}_k^f$ . This yields an aRMSE of 0.38 in test DA runs, unsurprisingly close to the 0.40 of our 3D-Var. Hence, learning an optimal constant-in-time  $\mathbf{K}$  of an (En)KF<sup>30</sup>, a configuration subsumed by this specific  $a_\theta$ , is significantly suboptimal in this context.

##### B. Estimation of the Kalman gain and error covariances

Once  $a_\theta$  has been obtained from training, and considering a fixed background state  $\mathbf{x}$  at a given time step, a large set of innovations  $\{\delta_j\}_{j=1 \dots N_p}$  are sampled from the observation error statistics:  $\delta_j \sim N(\mathbf{0}, \mathbf{R})$ . This yields a set of corresponding incremental updates  $\{\mathbf{a}_j = a_\theta(\mathbf{x}, \mathbf{H}^\top \mathbf{R}^{-1} \delta_j)\}_{j=1 \dots N_p}$ . Since Eq. (7) is only an approximation,  $\mathbf{K}(\mathbf{x})$  is estimated with the least squares problem

$$\mathcal{L}_x(\mathbf{K}) = \sum_{j=1}^{N_p} \|\mathbf{a}_j - \bar{\mathbf{a}} - \mathbf{K}(\mathbf{x}) \cdot (\delta_j - \bar{\delta})\|^2, \quad (9)$$

where  $\bar{\mathbf{a}} = N_p^{-1} \sum_{j=1}^{N_p} \mathbf{a}_j$  and  $\bar{\delta} = N_p^{-1} \sum_{j=1}^{N_p} \delta_j$ .

Next, assuming  $\mathbf{R}$  is known, we would like to estimate the analysis  $\mathbf{P}^a$  and background  $\mathbf{B}$  error covariance matrices, associated to  $a_\theta$  in the Kalman gain interpretation. They depend on  $\mathbf{x}_k$  and hence on  $t_k$ . Given that  $\mathbf{K} \in \mathbb{R}^{N_x \times N_y}$ , it should not be possible to fully determine either  $\mathbf{P}^a$  or  $\mathbf{B}$ , unless  $\mathbf{H}$  is invertible. But we can access error covariances in observation space rather than in state space. Within the *best linear unbiased estimator* framework, it can be shown that

$$\mathbf{P}^a \mathbf{H}^\top = \mathbf{K} \mathbf{R}, \quad \mathbf{H} \mathbf{B} \mathbf{H}^\top = (\mathbf{I}_y - \mathbf{H} \mathbf{K})^{-1} \mathbf{H} \mathbf{K} \mathbf{R}. \quad (10)$$

Hence, one can estimate surrogates of  $\mathbf{P}^a \mathbf{H}^\top$  and of  $\mathbf{H} \mathbf{B} \mathbf{H}^\top$  for the learned  $a_\theta$  from the numerically estimated surrogate  $\mathbf{K}$ , at any time  $t_k$ . When  $\mathcal{H} = \mathbf{I}_x$  and  $\mathbf{R} = \mathbf{I}_x$ , these boil down to

$$\mathbf{P}^a = \mathbf{K}, \quad \mathbf{B} = (\mathbf{I}_x - \mathbf{K})^{-1} \mathbf{K}. \quad (11)$$

##### C. Numerical results

At each  $t_k$ , i.e. over many  $\mathbf{x}_k$  on the attractor of the dynamics, it is possible to estimate, the equivalent  $\mathbf{K}(\mathbf{x}_k)$ ,  $\mathbf{B}(\mathbf{x}_k)$ ,  $\mathbf{P}^a(\mathbf{x}_k)$  as seen from  $a_\theta$ . For the sake of simplicity,  $\mathcal{H} = \mathbf{I}_x$ ,  $\mathbf{R} = \mathbf{I}_x$  are chosen, such that Eq. (11) stands.

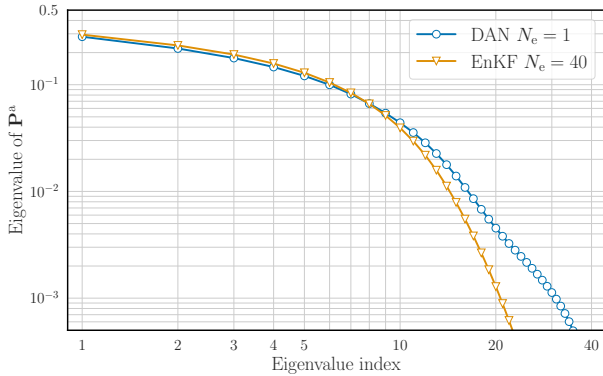


FIG. 1. Time-averaged eigenspectra of  $\mathbf{P}^a_{\text{DAN}}$  and  $\mathbf{P}^a_{\text{EnKF}}$ .

The analysis mean bias  $b$  and its standard deviation  $s$  are first computed over a long L96  $a_\theta$ -based DA run. We obtain  $b \simeq 5.10^{-3}$  and  $s \simeq 10^{-3}$  which are indeed very small compared to the typical aRMSE of an either DAN or EnKF run, i.e. 0.20, meaning that the bias of  $a_\theta$  relative to typical updates is roughly 2.5%.

The surrogate  $\mathbf{P}^a$ , denoted  $\mathbf{P}^a_{\text{DAN}}$  and estimated from Eq. (11), is compared to that of a concurrently running well-tuned EnKF with  $N_e = 40$ , whose analysis error covariance matrix is  $\mathbf{P}^a_{\text{EnKF}}$ .  $\mathbf{P}^a_{\text{DAN}}$  is compared to  $\mathbf{P}^a_{\text{EnKF}}$  using a normalized Bures-Wasserstein distance:<sup>47</sup>

$$d_{\text{BW}}(\mathbf{U}, \mathbf{V}) = \frac{1}{N_x} \left[ \text{Tr} \left\{ \mathbf{U} + \mathbf{V} - 2 \left( \mathbf{V}^{\frac{1}{2}} \mathbf{U} \mathbf{V}^{\frac{1}{2}} \right)^{\frac{1}{2}} \right\} \right]^{\frac{1}{2}}, \quad (12)$$

where  $\mathbf{U}$  and  $\mathbf{V}$  are two semi-definite symmetric matrices. This metric is expected to smoothly account for the unmatched principal axes of  $\mathbf{U}$  and  $\mathbf{V}$ , but also their associated variances (eigenspectra). The time-averaged  $d_{\text{BW}}$  distance between  $\mathbf{P}^a_{\text{DAN}}$  and  $\mathbf{P}^a_{\text{EnKF}}$  is 0.013 whereas it is 0.048 between  $\mathbf{P}^a_{\text{DAN}}$  and  $(0.40)^2 \mathbf{I}_x$ , which approximates  $\mathbf{P}^a$  of a well-tuned 3D-Var. Furthermore, the averaged-in-time eigenspectra of  $\mathbf{P}^a_{\text{DAN}}$  and  $\mathbf{P}^a_{\text{EnKF}}$  are plotted in Fig. 1. They are remarkably close to each other for the first 10 modes. Beyond these modes the  $a_\theta$  operator is likely to selectively apply some multiplicative inflation, as one would expect from such stable DA runs.

We further compute the principal angles<sup>14</sup> of the vector subspaces generated by the  $N_u = 14$  dominant eigenvalues of  $\mathbf{P}^a_{\text{DAN}}$  and of  $\mathbf{P}^a_{\text{EnKF}}$ . Recall that  $N_u = 14$  is the dimension of the L96  $\mathcal{U}$ . The principal angles are intrinsic to the relative position of these subspaces; they do not depend on any coordinate system used to parameterize them. This indicates how close the most unstable directions of  $\mathbf{P}^a_{\text{DAN}}$  and  $\mathbf{P}^a_{\text{EnKF}}$  are in state space. The principal angles are reported in Fig. 2. Overall, the simplex formed by the EnKF is on average the most aligned with  $\mathcal{U}$ .<sup>14</sup> The subspace spanned by the dominant axes of  $\mathbf{P}^a_{\text{DAN}}$  are also well aligned with  $\mathcal{U}$ , yet progressively diverges when incorporating less unstable directions. For comparison, the principal angles of  $\mathcal{U}$  with an isotropically randomly sampled  $N_u = 14$ -dimensional subspace are also computed.

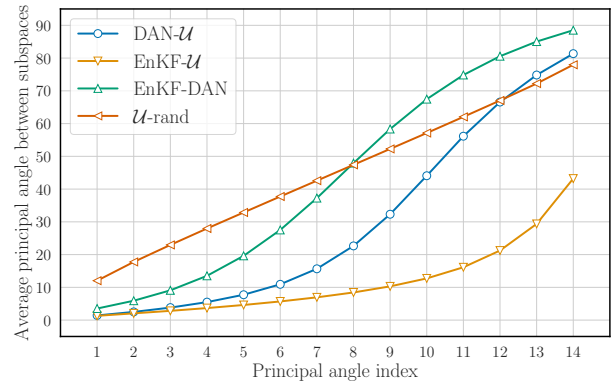


FIG. 2. Time-averaged principal angles (in degrees) formed by the subspaces spanned by the  $N_u = 14$  dominant directions of  $\mathbf{P}^a_{\text{DAN}}$  versus  $\mathcal{U}$ ,  $\mathbf{P}^a_{\text{EnKF}}$  versus  $\mathcal{U}$ ,  $\mathbf{P}^a_{\text{DAN}}$  versus  $\mathbf{P}^a_{\text{EnKF}}$ , and  $\mathcal{U}$  versus a randomly sampled  $N_u = 14$ -dimensional subspace.

#### D. Main interpretation

These numerical results indicate that  $a_\theta$  defined through Eq. (2a), depends on the innovation, but also on the single forecast state when  $N_e = 1$ . This does not hold for the EnKF incremental update which only indirectly depends on the forecast state via the ensemble-based forecast error covariances. Hence, without the need of an ensemble,  $a_\theta$  extracts from the forecast state critical pieces of information on the unstable directions, as shown by the principal angles experiment.

Furthermore,  $a_\theta$  manages to accurately assess the uncertainty attached to these unstable directions as demonstrated by the spectra of  $\mathbf{P}^a_{\text{DAN}}$ . Overall,  $\mathbf{P}^a_{\text{DAN}}$  with  $N_e = 1$  is on average very close to  $\mathbf{P}^a_{\text{EnKF}}$  with  $N_e = 40$ , for the dominant axes, and it applies some inflation onto the less unstable modes as seen by comparing their spectra.<sup>41</sup> We conclude that  $a_\theta$  directly learns about the dynamics features, as opposed to the regression-based, purely statistical, update in the EnKF.

Essentially, for  $a_\theta$ , critical pieces of information of the forecast error covariances of the DA run are encoded, and thus exploitable, in the forecast state alone. From the multiplicative ergodic theorem,<sup>48</sup> we know that, in autonomous ergodic dynamical systems such as  $\mathcal{M}$ , there exists a mapping between each of the system's states and the corresponding Lyapunov covariant vectors. Further, if the DA run (the forecast and analysis cycle) is considered as an ergodic dynamical system of its own,<sup>39</sup> the same theorem guarantees the existence of a mapping between the forecast state and the analysis error covariance matrix that  $a_\theta$  guesses. The DA process is not autonomous because it indirectly depends on the truth trajectory, the observation noise, and the observation operators; but a generalized variant of the multiplicative ergodic theorem for non-autonomous random dynamics should be applicable.<sup>49-52</sup> Hence, we conjecture that  $a_\theta$  must learn such mapping, together with how to process this information and combine it with the innovation.

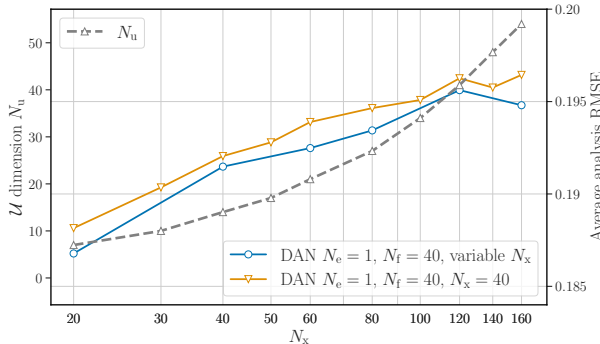


FIG. 3. Test aRMSEs of  $a_\theta$  operators learned from either L96 models with varying  $N_x$ , or learned from the  $N_x = 40$  L96 model but applied to varying  $N_x$  L96 models. The dimension  $N_u$  of  $\mathcal{U}$  is much steeper compared to the slowly increasing aRMSE curves.

### E. Locality and scalability

Next, we have trained  $a_\theta$  on the L96 model, using the reference configuration, but with a changing state space dimension  $N_x$  in between 20 and 160. The aRMSEs of well-tuned EnKFs for the changing  $N_x$ , and picking  $N_e = N_x$ , has been computed for comparison. The test DAN aRMSEs shows no significant dependence on  $N_x$  and are all within 5% of the EnKFs. Hence, because the performance of  $a_\theta$  with an unchanged architecture and number of parameters is barely affected by increasing  $N_x$ , we conjecture that the learned analysis extracts *local* pieces of information from the forecast state.

If true, the  $a_\theta$  operator learned for DA on an  $N_x = 40$  L96 model could be applied directly to an L96 DA run with a different  $N_x$ . Recall that the L96 states typically exhibit local highs and lows of Rossby-like waves, whose number scales linearly with  $N_x$ . Thus as long as the spatial extent of those waves is captured by the receptive field of the CNN, the same layers of  $a_\theta$  with the same weights and biases might be able to handle L96 states of distinct dimensionality.

To test this hypothesis, we use the same  $a_\theta$  operator (same weights and biases) learned as before with  $N_e = 1, N_x = 40$  but apply it to L96 models with  $N_x$  ranging from 20 to 160. The corresponding aRMSEs are reported in Fig. 3. This *transdimensional transfer* works surprisingly well: the aRMSEs are roughly the same for all  $N_x$  (between 0.188 and 0.197). This strongly supports the fact that  $a_\theta$  extracts local information from the forecast state (of various dimension in this experiment), relying on its convolution layers. It is therefore able to capture where, in phase-space, the error mass is concentrated. These localized error structures should be related to the *localization* of the dominant covariant Lyapunov vectors.<sup>53–55</sup>

## V. CONCLUSIONS

We have demonstrated on the L96 chaotic model that a learned DL-based analysis  $a_\theta$ , key part of a sequential DA scheme, can be almost as accurate as the best possibly tuned EnKF, the benchmark for ensemble filtering methods in this

model. More importantly, this learned DA scheme does not require any ensemble and can equally well rely on a single state forecast. Therefore,  $a_\theta$  can presumably read local patterns, that are representative of unstable and uncertain modes, from the forecast state alone. We believe that this is fundamentally made possible by some multiplicative ergodic theorem applied to sequential DA seen as a non-autonomous random dynamical system driven by time-dependent true dynamics and observation operators, and white-in-time observation errors.

To make sure our conclusions were not entirely bound to the L96 model, we carried out a large number of similar experiments on the well-known chaotic Kuramoto-Sivashinsky model.<sup>56,57</sup> They all confirm and support these conclusions.

What is achieved by  $a_\theta$  resonates with the *parametric EnKF*,<sup>58,59</sup> which encodes the errors of the day in a couple of dynamical ancillary fields, preventing the use of an ensemble. Amazingly, the learned  $a_\theta$  exhibited here is even more radical and extracts that information from the state itself.

Taking a step back, we learned from DL that an accurate and efficient DA analysis operator could capture the dynamical error without an ensemble, leveraging model-specific information. This argues in favor of rethinking popular sequential DA schemes for chaotic dynamics.

## ACKNOWLEDGMENTS

The authors acknowledge the support of the project SASIP (grant no. 353) funded by Schmidt Sciences – a philanthropic initiative that seeks to improve societal outcomes through the development of emerging science and technologies. Cerea is a member of Institut Pierre-Simon Laplace (IPSL).

## DATA AVAILABILITY STATEMENT

No datasets were used in this article.

## Appendix A: Architecture of the analysis operator

The learned operator  $a_\theta$  predicts the analysis increment to be added to the forecast/background ensemble, following Eq. (2). The architecture of the network is a basic residual CNN. It begins with an initial convolution that takes  $N_e + 1$  channels as inputs and, with  $N_f$  filters, outputs  $N_f$  channels. This initial layer is followed by  $N_b$  residual blocks. Each one of these blocks is a succession of  $N_{sb}$  sub-blocks. Each sub-block is made of: (i) a convolutional layer with  $N_f$  channels as inputs, has  $N_f$  filters and a kernel size for each of its filter of  $f_v$ , (ii) a batch normalization layer, and (iii) an activation function chosen to be mish.<sup>60</sup> The CNN finishes with a final convolutional layer that takes  $N_f$  channels as inputs and, with  $N_e$  filters, outputs  $N_e$  channels. The kernel size of the initial and final channels is  $f_v$ . A schematic of the CNN architecture is displayed in Fig. 4. The reference configuration,  $N_f = 40$ ,  $N_b = 5$ , and  $N_{sb} = 5$ , has about  $2 \times 10^5$  trainable parameters.

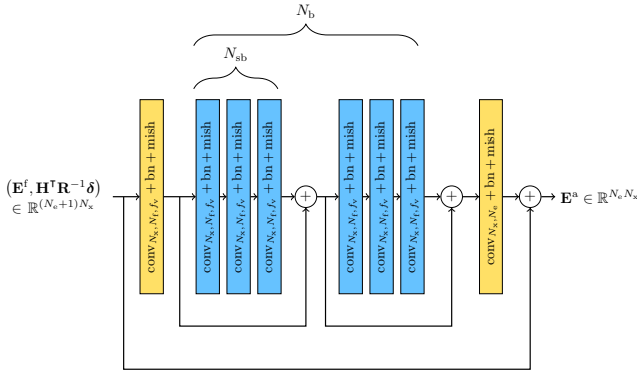


FIG. 4. Architecture of the residual convolutional network, where  $N_b = 2$ ,  $N_{sb} = 3$ .  $\text{conv}_{N_1, N_2, f}$  is a generic one-dimensional convolutional layer of dimension  $N_1$ , with  $N_2$  filters of kernel size  $f$ .

- <sup>1</sup>A. Carrassi, M. Bocquet, L. Bertino, and G. Evensen, “Data assimilation in the geosciences: An overview on methods, issues, and perspectives,” *WIREs Climate Change* **9**, e535 (2018).
- <sup>2</sup>M. Asch, M. Bocquet, and M. Nodet, *Data Assimilation: Methods, Algorithms, and Applications*, Fundamentals of Algorithms (SIAM, Philadelphia, 2016) p. 324.
- <sup>3</sup>E. N. Lorenz and K. A. Emanuel, “Optimal sites for supplementary weather observations: simulation with a small model,” *J. Atmos. Sci.* **55**, 399–414 (1998).
- <sup>4</sup>M. Bocquet and P. Sakov, “Joint state and parameter estimation with an iterative ensemble Kalman smoother,” *Nonlin. Processes Geophys.* **20**, 803–818 (2013).
- <sup>5</sup>L. Raynaud, L. Berre, and G. Desroziers, “Accounting for model error in the Météo-France ensemble data assimilation system,” *Q. J. R. Meteorol. Soc.* **138**, 249–262 (2012).
- <sup>6</sup>M. Bonavita, L. Isaksen, and E. Hólm, “On the use of EDA background error variances in the ECMWF 4D-Var,” *Q. J. R. Meteorol. Soc.* **138**, 1540–1559 (2012).
- <sup>7</sup>G. Evensen, *Data Assimilation: The Ensemble Kalman Filter*, 2nd ed. (Springer-Verlag Berlin Heidelberg, 2009) p. 307.
- <sup>8</sup>A. Carrassi, S. Vannitsem, D. Zupanski, , and M. Zupanski, “The maximum likelihood ensemble filter performances in chaotic systems,” *Tellus A* **61**, 587–600 (2008).
- <sup>9</sup>L. Palatella, A. Carrassi, and A. Trevisan, “Lyapunov vectors and assimilation in the unstable subspace: theory and applications,” *J. Phys. A: Math. Theor.* **46**, 254020 (2013).
- <sup>10</sup>K. S. Gurumoorthy, C. Grudzien, A. Apte, A. Carrassi, and C. K. R. T. Jones, “Rank deficiency of Kalman error covariance matrices in linear time-varying system with deterministic evolution,” *SIAM J. Control Optim.* **55**, 741–759 (2017).
- <sup>11</sup>M. Bocquet, K. S. Gurumoorthy, A. Apte, A. Carrassi, C. Grudzien, and C. K. R. T. Jones, “Degenerate Kalman filter error covariances and their convergence onto the unstable subspace,” *SIAM/ASA J. Uncertain. Quantif.* **5**, 304–333 (2017).
- <sup>12</sup>D. Crisan and M. Ghil, “Asymptotic behavior of the forecast–assimilation process with unstable dynamics,” *Chaos* **33** (2023), 10.1063/5.0105590.
- <sup>13</sup>B. Legras and R. Vautard, “A guide to lyapunov vectors,” in *ECMWF Workshop on Predictability* (ECMWF, Reading, United-Kingdom, 1996) pp. 135–146.
- <sup>14</sup>M. Bocquet and A. Carrassi, “Four-dimensional ensemble variational data assimilation and the unstable subspace,” *Tellus A* **69**, 1304504 (2017).
- <sup>15</sup>Y. Chen, A. Carrassi, and V. Lucarini, “Inferring the instability of a dynamical system from the skill of data assimilation exercises,” *Nonlin. Processes Geophys.* , 633–649 (2021).
- <sup>16</sup>A. Carrassi, M. Bocquet, J. Demaeyer, C. Gruzen, P. N. Raanes, and S. Vannitsem, “Data assimilation for chaotic dynamics,” in *Data Assimilation for Atmospheric, Oceanic and Hydrologic Applications (Vol. IV)*, edited by S. K. P. and L. X. (Springer International Publishing, Cham, 2022) pp. 1–42.
- <sup>17</sup>S. Cheng, C. Quilodran-Casas, S. Ouala, A. Farchi, C. Liu, P. Tandeo, R. Fablet, D. Lucor, B. Iooss, J. Brajard, D. Xiao, T. Janjic, W. Ding, Y. Guo, A. Carrassi, M. Bocquet, and R. Arcucci, “Machine learning with data assimilation and uncertainty quantification for dynamical systems: a review,” *IEEE/CAA J. Autom. Sin.* **10**, 1361–1387 (2023).
- <sup>18</sup>T. P. Härter and H. F. de Campos Velho, “Data assimilation procedure by recurrent neural network,” *Eng. Appl. Comput. Fluid Mech.* **6**, 224–233 (2012).
- <sup>19</sup>R. S. Cintra and H. F. de Campos Velho, “Data assimilation by artificial neural networks for an atmospheric general circulation model,” in *Advanced applications for artificial neural networks*, edited by A. ElShahat (IntechOpen, 2018) Chap. 17, pp. 265–286.
- <sup>20</sup>R. Fablet, B. Chapron, L. Drumetz, E. Mémin, O. Pannekoucke, and F. Rousseau, “Learning variational data assimilation models and solvers,” *J. Adv. Model. Earth Syst.* **13**, e2021MS002572 (2021).
- <sup>21</sup>T. Frerix, D. Kochkov, J. Smith, D. Cremers, M. Brenner, and S. Hoyer, “Variational data assimilation with a learned inverse observation operator,” in *Proceedings of the 38th International Conference on Machine Learning*, Proceedings of Machine Learning Research, Vol. 139, edited by M. Meila and T. Zhang (PMLR, 2021) pp. 3449–3458.
- <sup>22</sup>N. Lafon, R. Fablet, and P. Naveau, “Uncertainty quantification when learning dynamical models and solvers with variational methods,” *J. Adv. Model. Earth Syst.* **15**, e2022MS003446 (2023).
- <sup>23</sup>A. Filoche, J. Brajard, A. Charantonis, and D. Béreziat, “Learning 4DVAR inversion directly from observations,” in *Computational Science – ICCS 2023*, edited by J. Mikyška, C. de Matalier, M. Paszynski, V. V. Krzhizhanovskaya, J. J. Dongarra, and P. M. Sloot (Springer Nature Switzerland, Cham, 2023) pp. 414–421.
- <sup>24</sup>J. D. Keller and R. Potthast, “AI-based data assimilation: Learning the functional of analysis estimation,” (2024), arXiv:2406.00390 [physics.ao-ph].
- <sup>25</sup>P. Boudier, A. Fillion, S. Gratton, S. Gürol, and S. Zhang, “Data assimilation networks,” *J. Adv. Model. Earth Syst.* **15**, e2022MS003353 (2023).
- <sup>26</sup>H. Hoang, P. De Mey, and O. Talagrand, “A simple adaptive algorithm of stochastic approximation type for system parameter and state estimation,” in *Proceedings of 1994 33rd IEEE Conference on Decision and Control*, Vol. 1 (1994) pp. 747–752 vol.1.
- <sup>27</sup>S. Hoang, R. Baraille, O. Talagrand, X. Carton, and P. De Mey, “Adaptive filtering: application to satellite data assimilation in oceanography,” *Dynam. Atmos. Ocean* **27**, 257–281 (1998).
- <sup>28</sup>T. Haarnoja, A. Ajay, S. Levine, and P. Abbeel, “Backprop KF: Learning discriminative deterministic state estimators,” in *Advances in Neural Information Processing Systems*, Vol. 29, edited by D. Lee, M. Sugiyama, U. Luxburg, I. Guyon, and R. Garnett (Curran Associates, Inc., 2016).
- <sup>29</sup>Y. Chen, D. Sanz-Alonso, and R. Willett, “Autodifferentiable ensemble kalman filters,” *SIAM J. Math. Data Sci.* **4**, 801–833 (2022).
- <sup>30</sup>E. Luk, E. Bach, R. Baptista, and A. Stuart, “Learning optimal filters using variational inference,” (2024), arXiv:2406.18066 [cs.LG].
- <sup>31</sup>M. McCabe and J. Brown, “Learning to assimilate in chaotic dynamical systems,” in *Advances in Neural Information Processing Systems*, Vol. 34, edited by M. Ranzato, A. Beygelzimer, Y. Dauphin, P. Liang, and J. W. Vaughan (Curran Associates, Inc., 2021) pp. 12237–12250.
- <sup>32</sup>A. McNally, C. Lessig, P. Lean, E. Boucher, M. Alexe, E. Pinnington, M. Chantry, S. Lang, C. Burrows, M. Chryst, F. Pinault, E. Villeneuve, N. Bormann, and S. Healy, “Data driven weather forecasts trained and initialised directly from observations,” (2024), arXiv:2407.15586 [physics.ao-ph].
- <sup>33</sup>A. Vaughan, S. Markou, W. Tebbutt, J. Requeima, W. P. Bruinsma, T. R. Andersson, M. Herzog, N. D. Lane, M. Chantry, J. S. Hosking, and R. E. Turner, “Aardvark weather: end-to-end data-driven weather forecasting,” (2024), arXiv:2404.00411 [physics.ao-ph].
- <sup>34</sup>M. Bocquet, J. Brajard, A. Carrassi, and L. Bertino, “Data assimilation as a learning tool to infer ordinary differential equation representations of dynamical models,” *Nonlin. Processes Geophys.* **26**, 143–162 (2019).
- <sup>35</sup>J. Brajard, A. Carrassi, M. Bocquet, and L. Bertino, “Combining data assimilation and machine learning to emulate a dynamical model from sparse and noisy observations: a case study with the Lorenz 96 model,” *J. Comput. Sci.* **44**, 101171 (2020).
- <sup>36</sup>D. P. Kingma and J. Ba, “Adam: A method for stochastic optimization,” in *International Conference on Learning Representations (ICLR)* (San Diego, CA, USA, 2015).

<sup>37</sup>H. Tang and J. Glass, “On training recurrent networks with truncated back-propagation through time in speech recognition,” in *2018 IEEE Spoken Language Technology Workshop (SLT)* (2018) pp. 48–55.

<sup>38</sup>C. Aicher, N. J. Foti, and E. B. Fox, “Adaptively truncating backpropagation through time to control gradient bias,” in *Proceedings of The 35th Uncertainty in Artificial Intelligence Conference*, Proceedings of Machine Learning Research, Vol. 115, edited by R. P. Adams and V. Gogate (PMLR, 2020) pp. 799–808.

<sup>39</sup>A. Carrassi, M. Ghil, A. Trevisan, and F. Ubaldi, “Data assimilation as a nonlinear dynamical systems problem: Stability and convergence of the prediction-assimilation system,” *Chaos* **18**, 023112 (2008).

<sup>40</sup>A. Carrassi, A. Trevisan, L. Descamps, O. Talagrand, and F. Ubaldi, “Controlling instabilities along a 3DVar analysis cycle by assimilating in the unstable subspace: a comparison with the EnKF,” *Nonlin. Processes Geophys.* **15**, 503–521 (2008).

<sup>41</sup>M. Bocquet, P. N. Raanes, and A. Hannart, “Expanding the validity of the ensemble Kalman filter without the intrinsic need for inflation,” *Nonlin. Processes Geophys.* **22**, 645–662 (2015).

<sup>42</sup>P. N. Raanes, M. Bocquet, and A. Carrassi, “Adaptive covariance inflation in the ensemble Kalman filter by Gaussian scale mixtures,” *Q. J. R. Meteorol. Soc.* **145**, 53–75 (2019).

<sup>43</sup>J. van Amersfoort, L. Smith, A. Jesson, O. Key, and Y. Gal, “On feature collapse and deep kernel learning for single forward pass uncertainty,” (2022), arXiv:2102.11409 [cs.LG].

<sup>44</sup>M. Peyron, A. Fillion, S. Gürol, V. Marchais, S. Gratton, P. Boudier, and G. Goret, “Latent space data assimilation by using deep learning,” *Q. J. R. Meteorol. Soc.* **147**, 3759–3777 (2021).

<sup>45</sup>R. E. Kalman, “A new approach to linear filtering and prediction problems,” *J. Basic Eng.* **82**, 35–45 (1960).

<sup>46</sup>M. Ghil and P. Malanotte-Rizzoli, “Data assimilation in meteorology and oceanography,” *Advanc. in Geophys.* **33**, 141–266 (1991).

<sup>47</sup>R. Bhatia, T. Jain, and Y. Lim, “On the Bures-Wasserstein distance between positive definite matrices,” *Expo. Math.* **37**, 165–191 (2019).

<sup>48</sup>V. I. Oseledec, “A multiplicative ergodic theorem. Lyapunov characteristic numbers for dynamical systems,” *Trans. Moscow Math Soc.* **19**, 197–231 (1968).

<sup>49</sup>L. Arnold, *Random Dynamical Systems* (Springer Berlin, Heidelberg, 1998) p. 586.

<sup>50</sup>M. D. Chekroun, E. Simonnet, and M. Ghil, “Stochastic climate dynamics: Random attractors and time-dependent invariant measures,” *Physica D* **240**, 1685–1700 (2011).

<sup>51</sup>F. Flandoli and E. Tonello, “An introduction to random dynamical systems for climate,” (2021).

<sup>52</sup>M. Ghil and D. Sciambarella, “Review article: Dynamical systems, algebraic topology and the climate sciences,” *Nonlin. Processes Geophys.* , 399–434 (2023).

<sup>53</sup>D. Pazó, M. A. Rodríguez, and J. M. López, “Spatio-temporal evolution of perturbations in ensembles initialized by bred, Lyapunov and singular vectors,” *Tellus A* **62**, 10–23 (2010).

<sup>54</sup>S. Vannitsem and V. Lucarini, “Statistical and dynamical properties of covariant Lyapunov vectors in a coupled atmosphere-ocean model-multiscale effects, geometric degeneracy, and error dynamics,” *J. Phys. A: Math. Theor.* **49**, 224001 (2016).

<sup>55</sup>B. Giggins and G. A. Gottwald, “Stochastically perturbed bred vectors in multi-scale systems,” *Q. J. R. Meteorol. Soc.* **145**, 642–658 (2019).

<sup>56</sup>Y. Kuramoto and T. Tsuzuki, “Persistent propagation of concentration waves in dissipative media far from thermal equilibrium,” *Progr. Theoret. Phys.* **55**, 356–369 (1976).

<sup>57</sup>G. I. Sivashinsky, “Nonlinear analysis of hydrodynamic instability in laminar flames-I. Derivation of basic equations,” *Acta Astronaut.* **4**, 1177–1206 (1977).

<sup>58</sup>O. Pannekoucke, S. Ricci, S. Barthelemy, R. Ménard, and O. Thual, “Parametric Kalman filter for chemical transport model,” *Tellus A* **68**, 31457 (2016).

<sup>59</sup>O. Pannekoucke, M. Bocquet, and R. Ménard, “Parametric covariance dynamics for the nonlinear diffusive Burgers equation,” *Nonlin. Processes Geophys.* **25**, 481–495 (2018).

<sup>60</sup>D. Misra, “Mish: A self regularized non-monotonic neural activation function,” arXiv (2019), 10.48550/arXiv.1908.08681.